Magnetostriction of Electrical Steel Sheet Under Different Magnetization Conditions

Yanli Zhang, Qiang Li, Dianhai Zhang, Ziyan Ren, Baodong Bai, Dexin Xie

School of Electrical Engineering, Shenyang University of Technology, Liaoning 110870, China, zhangyanli_sy@hotmail.com

Magnetostriction in non-oriented (NO) and grain-oriented (GO) electrical steel is a main source of vibration of iron cores in electrical machines and transformers. This paper presents the effect of different magnetization conditions, such as direct current biased magnetic field and higher harmonic field, on magnetostriction of a long strip of electrical steel sheet based on a one-dimensional (1-D) magnetostriction tester. The anisotropy of magnetostriction and the relation between principal strain and magnetic flux density was made clear by means of measured data. A vector model was proposed to describe the relationship mentioned above, and was applied to the magnetostrictive analysis of a synchronous machine.

***Index Terms*—Magnetostriction, harmonic analysis, soft magnetic materials, magnetization, finite element analysis.**

I. Introduction

THE magnetostrictive phenomenon of non-oriented (NO) electrical steel and grain-oriented (GO) electrical steel has aroused the attention in recent years. It has been reported that magnetostriction of electrical steel is one of the main sources causing deformation and vibration in rotational machine and transformer cores [1-3]. Some significant research work has been conducted on the anisotropic magnetostriction under the alternating and rotational magnetization with a two-dimensional (2-D) magnetic measurement system [4-6], in which the sample was cut into square shape.

This paper investigates the behaviors of vector magnetostriction for a long strip of NO and GO electrical steel sheet under different magnetization conditions, such as alternating magnetic flux along different directions, direct current (DC) biased magnetic field, and higher harmonic magnetic field. A three-axial strain gauge is developed to measure the principal strain of magnetostriction. A model based on measurement data is used to describe the vector relationship between principal strain and magnetic flux density, and is applied to the magnetostriction simulation of a synchronous motor.

II. Measurement and Analysis of Principal Strain

A. *Magnetostriction measurement system*

Fig. 1 shows a one-dimensional (1-D) magnetostriction measurement system, in which the induced magnetic flux density B is controlled as sinusoidal waveform from 0.5 T to 1.8T, 50 Hz, the three-axial strain gauge is used to measure the strain at angles of 0°, 45°, and 90° to the rolling direction (RD). A long strip of electrical steel sheet with 500mm in length and 100mm in width is chosen as sample for purpose of reducing the effect of shearing force from mechanical processing on measurement results as few as possible.

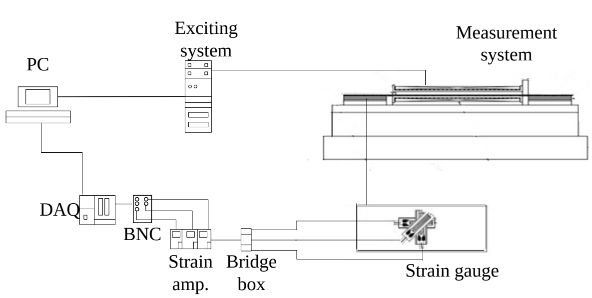

Fig.1 Magnetostriction measurement system

B. *Principal strain computation*

The in-plane magnetostriction $\lambda(\tau, \alpha)$, in an arbitrary direction, can be expressed as

$$\lambda(\tau,\ \alpha) = \frac{L}{\Delta L} = \varepsilon_x \cos^2\alpha + \varepsilon_y \sin^2\alpha + \gamma_{xy}\sin\alpha\cos\alpha \qquad (1)$$

where α is the angle to the RD, and $\tau=\omega t$. ε_x and ε_y are linear strains, and γ_{xy} is shear strain, which can be calculated by,

$$\begin{pmatrix}\varepsilon_x\\ \varepsilon_y\\ \gamma_{xy}\end{pmatrix} = \begin{bmatrix}\cos^2\theta_a & \sin^2\theta_a & \sin\theta_a\cos\theta_a\\ \cos^2\theta_b & \sin^2\theta_b & \sin\theta_b\cos\theta_b\\ \cos^2\theta_c & \sin^2\theta_c & \sin\theta_c\cos\theta_c\end{bmatrix}^{-1}\begin{pmatrix}\lambda_a\\ \lambda_b\\ \lambda_c\end{pmatrix} \qquad (2)$$

where λ_a, λ_b and λ_c are measured by three-axial strain gauge in three directions chosen as $\theta_a=0^{\circ}$, $\theta_b=45^{\circ}$, and $\theta_c=90^{\circ}$. Thus, the elongation (λ_+) and contraction (λ_-) along principal strain axis can be expressed as

$$\lambda_+, \lambda_- = \frac{\varepsilon_x+\varepsilon_y}{2} \pm \sqrt{\left(\frac{\varepsilon_x-\varepsilon_y}{2}\right)^2 + \left(\frac{\gamma_{xy}}{2}\right)^2} \qquad (3)$$

The angle from the principal strain axis to the RD can be calculated from

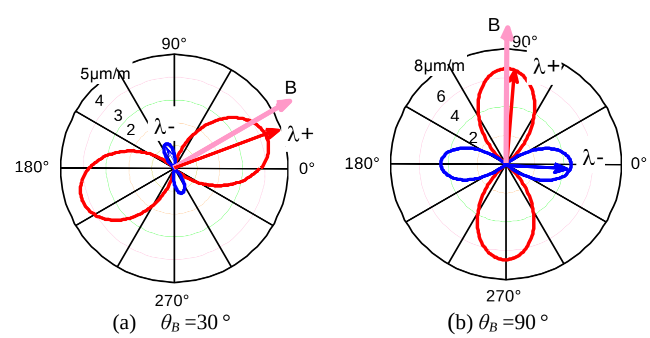

Fig.2 Principal strain of the NO electrical steel when B = 1.4T along two magnetization directions

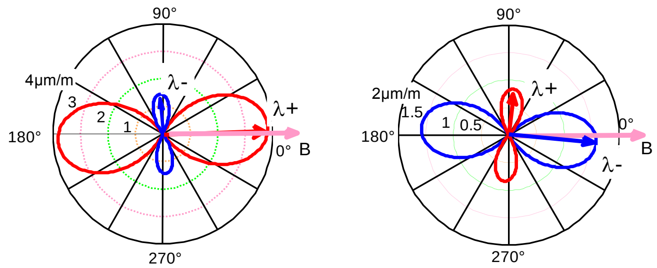

(a) Non-oriented steel (b) Grain-oriented steel

Fig.3 Principal strain when B = 1.4T and θ_B=0 ° for GO and NO electrical steel sheets

$$\theta = \frac{1}{2}\tan^{-1}\left(\frac{\gamma_{xy}}{\varepsilon_x - \varepsilon_y}\right) \tag{4}$$

C. Anisotropic magnetostriction along different magnetization directions

To magnetize the samples along different directions, the samples are cut at 15 ° intervals from the RD to the transverse direction (TD). Fig.2 shows calculated principal strain in one time period using experimental data which includes two elongation sectors and two contraction sectors when induction B = 1.4T. From this figure, we can see that the magnitude and direction of elongation principal strain vector λ_+ change with the variation of magnetization directions. Fig.3 illustrates that the GO and NO electrical steel sheet magnetized along the RD have different strain property, i.e. for NO steel the elongation along the RD is bigger than contraction of the TD, while for GO steel the bigger contraction of strain is along the RD.

D. Magnetostriction under higher harmonic magnetic field

For electrical machines, the laminated cores may work under magnetic field with higher harmonics. The effect of harmonic field on magnetostriction is also measured by controlling the induction B waveform with 3th harmonic accounting for 20% of fundamental one and phase delay of 30 °, as shown in Fig.4. Fig.4 (b) shows the Fourier analysis of magnetostriction waveform. It is shown that the 3th harmonic of induction B has a main effect on the 2th and 4th harmonics component of magnetostriction, and the high value of 4^{th} harmonic of magnetostriction is mainly driven by higher harmonic of magnetic field.

E. Magnetostriction under DC biased magnetic field

The transformer cores usually stands DC biased magnetic field, and Fig. 5 shows the measured principal strain λ_+ and λ_-

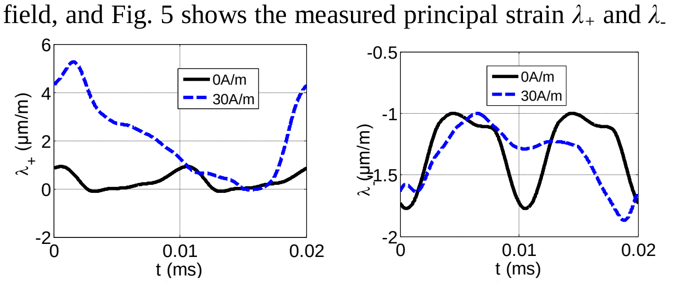

(a) elongation of strain along TD (b) contraction of strain along RD

Fig.5 Magnetostriction under DC biased magnetic field of 0 A/m and 30 A/m

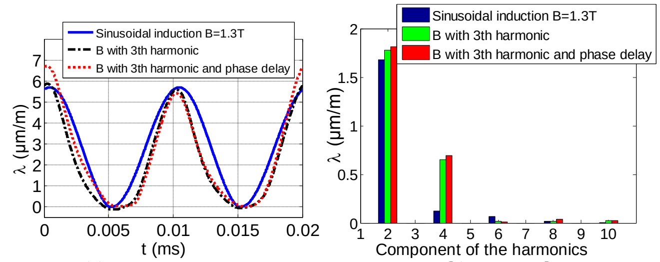

(a) magnetostrictive curves (b) FFT analysis

Fig.4 Effect of harmonic on magnetostriction along the TD

without and with 30 A/m biased field along the RD. We can see that the elongation along the TD increases obviously and the magnetostrictive waveform is not symmetrical any more.

III. Vector Model and Application

According to the anisotropic magnetostriction of electrical steel discussed above in this paper, the measured vector relationship between principal strain and magnetic flux density is illustrated with 2-D surface in Fig. 6 and can be described as

$$\begin{cases} \lambda = f(B, \theta_B) \\ \theta_\lambda = f(B, \theta_B) \end{cases} \tag{5}$$

where B and θ_B are the magnitude and direction of applied magnetic field, respectively, and λ and θ_λ are those of principal strain, respectively. The vector model is applied into the magnetostriction simulation of a synchronous motor as a result in Fig. 7, and the detailed discussion will be given in extended paper.

IV. References

[1] B. Weiser, H. Pfutzner, and J. Anger, "Relevance of magnetostriction and forces for the generation of audible noise of transformer cores," *IEEE Trans. Magn.*, vol. 36, no. 9, pp. 3759-3777, Sep. 2000.

[2] Belahcen, "Vibrations of rotating electrical machines due to magnetomechanical coupling and magnetostriction," *IEEE Trans. Magn.*, vol. 42, no. 4, pp. 971-974, Apr. 2006.

[3] L. Vandevelde and J. A. A. Melkebeek, "Magnetic forces and magnetostriction in electrical machines and transformer cores," *IEEE Trans. Magn.*, vol. 39, no. 5, pp. 1618-1621, May 2003.

[4] D. Wakabayashi, T. Todaka, and M. Enokizono, "Three-dimensional magnetostriction and vector magnetic properties under alternating magnetic flux conditions in arbitrary direction," *Electrical engineering in Japan*, vol. 179, no. 4, pp. 1-9, Apr. 2012.

[5] S. Somkun, A. J. Moses, P. I. Anderson, "Measurement and modeling of 2-D magnetostriction of non-oriented electrical steel," *IEEE Trans. Magn.*, vol. 48, no. 2, pp. 711-714, Tue. 2012.

[6] Y. Zhang, J. Wang, X. Sun, B. Bai and D. Xie, "Measurement and modeling of anisotropic magnetostriction characteristic of grain-oriented silicon steel sheet under DC bias," *IEEE Trans. Magn.*, vol. 50, no. 2, pp. 7008804, Tue. 2014.

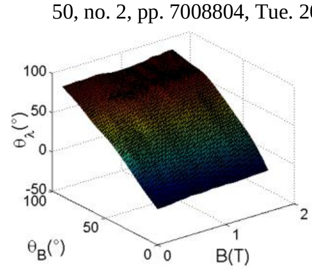

Fig.6 Relation between $\boldsymbol{B}$ and θ_λ

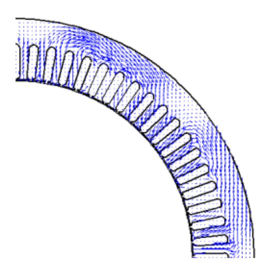
Fig.7 Magnetostriction simulation of a synchronous motor